

LINKING IN CYCLIC BRANCHED COVERS AND SATELLITE (NON)-HOMOMORPHISMS

PATRICIA CAHN AND ALEXANDRA KJUCHUKOVA

ABSTRACT. Let $K \subset S^3$ be a knot and $\eta, \gamma \subset S^3 \setminus K$ be simple closed curves. Denote by $\Sigma_q(K)$ the q -fold cyclic branched cover of K . We give an explicit formula for computing the linking numbers between lifts of η and γ to $\Sigma_q(K)$. As an application, we evaluate, in a variety of cases, an obstruction to satellite operations inducing homomorphisms on smooth concordance.

1. INTRODUCTION

Given two rationally null-homologous, disjoint curves in an oriented 3-manifold, their linking number $\text{lk}(\alpha, \beta) \in \mathbb{Q}$ is well-defined and symmetric [3]. Linking numbers in branched covers of S^3 were first computed by Reidemeister [18] and were one of the early methods for distinguishing knots. In the 1960s, Ken Perko wrote a computer program for computing linking numbers between the branch curves in 3-fold irregular branched covers [16] and used it to help complete the classification of knots through 10 crossings. The authors extended this technique to computing linking numbers, in 3-fold irregular covers, between “pseudo-branch curves”, that is, connected components of lifts to the branch cover of curves which lie in the complement of the branching set [7]. Perko’s computation of linking numbers between branch curves was also generalized to all odd-fold irregular dihedral covers in [4]. Linking numbers in branched covers can be used [6] to compute the Rokhlin μ invariant [8] and Kjuchukova’s Ξ_p invariant [12, 10], among other applications.

In this note, we give a formula for computing linking numbers between pseudo-branch curves in *cyclic* branched covers. As an application, we show, using an obstruction from [14], that certain satellite patterns do not induce homomorphisms on smooth concordance. We thus verify a conjecture of Hedden [1] for these patterns. Linking numbers of the types considered here can also detect satellite patterns of infinite rank, using [11].

There exist alternative methods for computing linking numbers in cyclic branched covers. Under the assumption that the linking numbers between the branch set and (projections of) the pseudo-branch curves are zero, formulas for the linking numbers are given in [17]. Additionally, a formula for linking numbers in a rational homology 3-sphere described by a Kirby diagram is provided in [9]. A method for passing between a diagram of the branching set and a Dehn surgery presentation of its cyclic cover is given in [2]; however, this gets gnarly as the degree of the cover or the Seifert genus of the branching set increases. In contrast, the input for our computation is a diagram of the branching set K (in S^3) and the curves of interest in the complement of K . The computation is not sensitive to the Seifert genus of K – see Example 3 in Section 5 – and makes no assumption about the linking numbers between the branch and pseudo-branch curves in S^3 . We have implemented our computation in [5], so the linking numbers can be calculated genuinely easily, even for high degree covers.

We include an abridged version of our result below, suppressing a lot of the notation used in the linking number formula. The full statement is deferred to Section 4. For ease of exposition, we first

Date: January 2023.

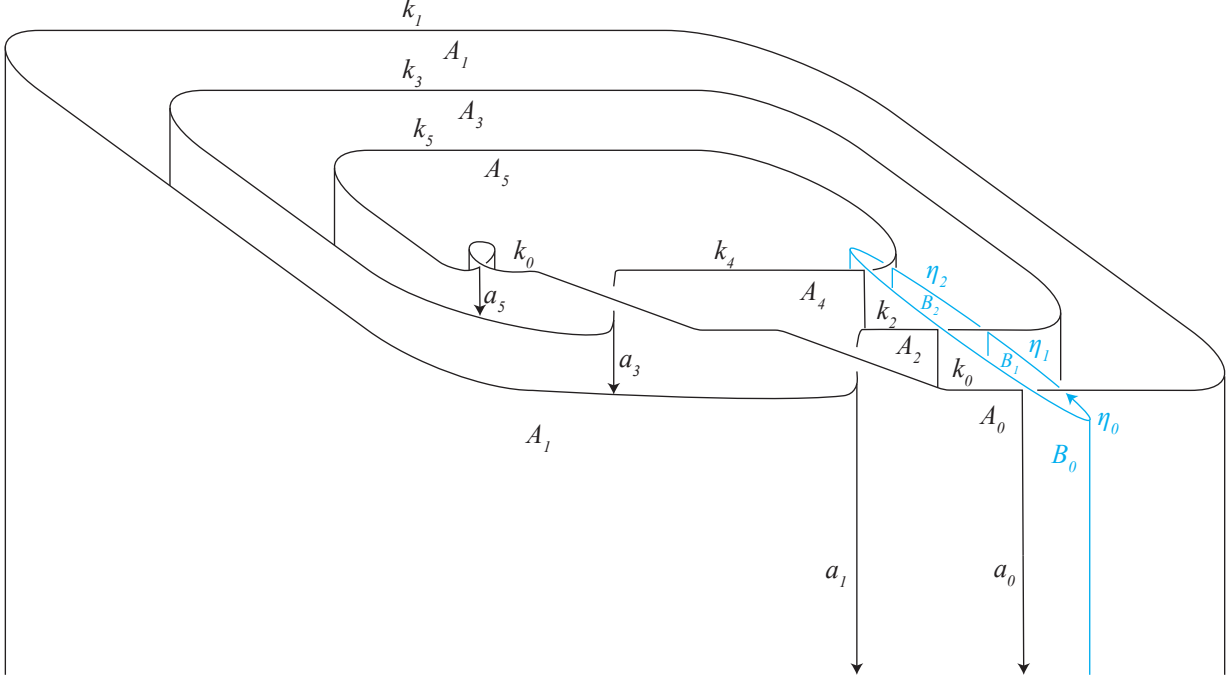


FIGURE 1. A cell structure on S^3 determined by the $(3,1)$ -cabling pattern, represented by a 2-component link $K \cup \eta$.

prove the theorem in Section 3, under an additional assumption on the linking numbers, in S^3 , of the pseudo-branch curves and the branch curve, as needed for our main application [14]. Note that we do not require that the cover be a rational homology sphere.

Theorem 1 (Main Theorem, Abridged). *Let $K \subset S^3$ be a knot. Denote by $\Sigma_q(K)$ the q -fold branched cover of K . We first determine whether each closed, connected component of the lifts of γ and η is rationally null-homologous in $\Sigma_q(K)$. When this is the case, the linking numbers between connected components of the lifts of γ and η in $\Sigma_q(K)$ can be computed by the formula in Equation 4. The input needed for performing the computation is contained in the Dowker-Thistlethwaite code for a diagram of $K \cup \gamma \cup \eta$.*

The notation needed to properly state (or apply) our theorem is introduced in Section 2, where we also describe the geometric construction used in the proof. Step by step instructions for how to use the computational tool provided in [5] are given in the appendix.

2. CELL STRUCTURE ON THE CYCLIC BRANCHED COVER OF A KNOT

We endow S^3 with a cell structure determined by the link $K \cup \eta$. Recall that K denotes the branching set and $\eta \subset S^3 \setminus K$ is a pseudo-branch curve. We then lift this cell structure to the branched cover $\Sigma_q(K)$. In this section, we describe this structure and introduce notation for the cells. Analogous cellular decompositions of the 3-sphere and its irregular dihedral covers are used in [16, 12, 6, 7].

Throughout this section, the reader should refer to Figure 1.

Let D be a diagram of $K \cup \eta$, regarded as a projection with double points. Consider $c(D)$, the cone on the diagram, illustrated in Figure 1 and described in terms of a cell structure in the following paragraphs. We describe a cell structure on S^3 in terms of D . The 0-cells are the cone point c and the double points c_j in D . (Each c_j is regarded as belonging to the understrand at this crossing.) Adopting the language used by Perko, we categorize the 1-cells as either *horizontal*, corresponding to strands in D , and *vertical*, which are the cones on the c_j . The 2-cells, called “walls”, are the cones on the horizontal 1-cells, and they are indexed by the strands d_i of D . The boundary of each 2-cell C^2 consists of: a single horizontal 1-cell d_i (where $C_i^2 = c(d_i)$); two vertical 1-cells, the cones on the endpoints of d_i ; additional pairs of vertical 1-cells, called “slits”, corresponding to crossings where d_i is the overstrand¹. The 2-skeleton of the cell structure on S^3 is illustrated in Figure 1, with the cone point regarded as a point at infinity. There is a single 3-cell, the complement of the cone.

We proceed to name the strands of D , the 1-cells and the 2-cells. We orient K and fix a 0-cell which we label c_0 . The remaining 0-cells on K get consecutive indices, proceeding in the direction of the orientation. The horizontal 1-cells which are strands of K are then labeled k_0, k_1, \dots, k_{n-1} , with $\partial(k_i) = c_{i+1} - c_i$. A remark on the number of strands: in order to simplify labeling the lifts of two-cells later, we henceforth assume that the writhe of K is $0 \pmod q$, after performing some Reidemeister-I moves if necessary. We also orient η and number the horizontal 1-cells which are strands of η in the analogous manner: $\eta_0, \eta_1, \dots, \eta_{m-1}$. If c_i is a point on K , the vertical 1-cell whose boundary is $c - c_i$ is labeled a_i . If c_i is a point on η , the vertical 1-cell whose boundary is $c - c_i$ is labeled b_i . The 2-cell whose horizontal boundary is k_i will be denoted by A_i . The 2-cell whose horizontal boundary is η_i will be denoted by B_i . We orient each 2-cell so that $\partial(A_i) = k_i + a_{i+1} - a_i$ and $\partial(B_i) = \eta_i + b_{i+1} - b_i$. There’s a single 3-cell (whose interior is the complement of the cone) denoted E .

We now describe the induced cell structure on $\Sigma_q(K)$. Each strand k_i has a single lift, which we also denote by k_i . Every 0-, 1-, 2- and 3-cell whose interior is contained in $S^3 \setminus K$ has q lifts, labeled in the natural way: the lifts of a_i are a_i^1, \dots, a_i^q ; of A_i are A_i^1, \dots, A_i^q ; analogously for the η_i and B_i ; the 3-cells in $\Sigma_q(K)$ are E^1, \dots, E^q . Some of the notation can be chosen freely, and the rest is determined by the given diagram of $K \cup \eta$. We assign superscripts in such a way that $\partial(A_i^j) = k_i^j + a_{i+1}^j - a_i^j + \dots$ and $\partial(B_i^j) = \eta_i^j + \dots$. (It is to be understood that these 1-cells do not appear again in the rest of the chain, that is, the coefficient of k_i^j in $\partial(A_i^j)$ is precisely 1, etc..) Remark also that the 1-cell k_i belongs to the boundary of A_i^j for all j . For a fixed i , we let the superscripts of the cells A_i^j increase in the clockwise direction (if the orientation of the knot points into the page). Put differently, if an Ambler² walking around $\Sigma_q(K)$ stands on A_i^j , with the cell a_i^j to his left, and faces in the direction of the orientation of K , then the 2-cell to his left is A_i^{j-1} . See Figure 2. Now let the Ambler continue along a push-off of K until he crosses a wall (that is, a 2-cell whose horizontal boundary is a lift of the overstrand at crossing c_i). After crossing the wall, the strand to the left of the Ambler is k_{i+1} and the 2-cell he’s walking on is an A_{i+1}^s for some value of s . We pick our convention so that $s = j$, that is, the superscripts remain unchanged when passing through a wall. See Figure 4. However, each time a wall A_i^j is crossed, the ambient 3-cell changes, since the meridian of the horizontal boundary of A_i permutes the 3-cells. (Passing through a wall B_i^j , whose horizontal boundary is a lift of η , does not change the ambient 3-cell.)

¹The “slits” are part of the attaching map of the 2-cell. They come in canceling pairs so do not contribute to the 1-chain ∂C_i^2 . However, the presence of slits does sometimes contribute to the 1-chains bounded by lifts of C_i^2 .

²A convenient visualization device introduced, under another name, by Perko [16].

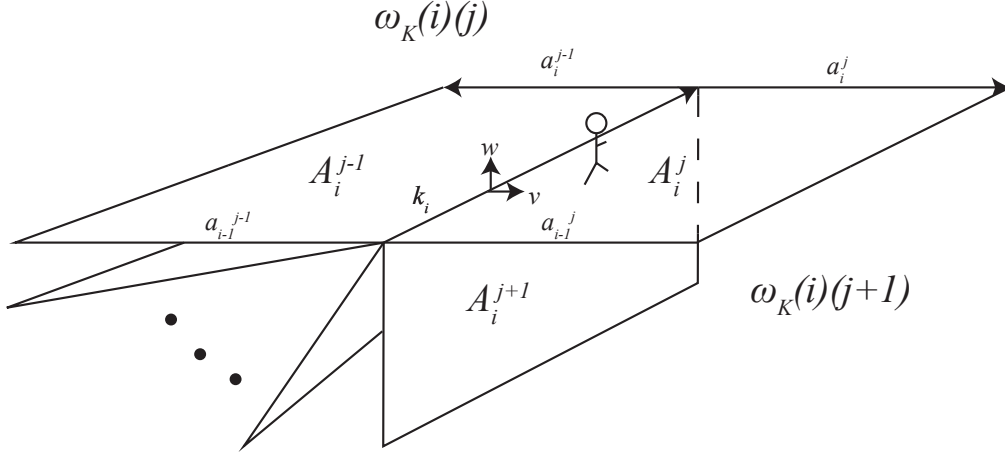


FIGURE 2. Roladex of lifts of the cell A_i . The Ambler is on A_i^j with k_i to his left. His head is in the 3-cell $E^{\omega_K(i)(j)}$. Throughout, we assume that the Ambler is oriented positively with respect to A_i^j . That is, these vectors v , pointing to the Ambler's right, and w , pointing from the Ambler's feet to head, together with the tangent vector to k_i , form a positive frame.

In summary, each 2-cell in S^3 labeled A_i has q lifts, A_i^1, \dots, A_i^q , to $\Sigma_q(K)$. These 2-cells all share a boundary arc, k_i . For a fixed i , the superscripts of the cells A_i^j increase when going along a positively oriented meridian of the arc k_i , see Figure 2. Furthermore, standing on A_i^j and moving along a push-off of k_i , after passing through a 2-cell, the Ambler is on A_{i+1}^j . Some labels of 2-cells are illustrated in Figure 4.

Next, we number the 3-cells of $\Sigma_q(K)$. Suppose the Ambler stands on a push-off of K into A_0^j , with the 1-cell K_0 to his left and facing in the direction of the orientation of K . We label the 3-cell his head is by E^j . In addition, we assume that the subscript denoting the 3-cell increases clockwise when passing through a 2-cell which bounds K_0 , see Figure 2. This choice, made around the 1-cell K_0 , in fact determines the positions of all 3-cells with respect to the entire 2-skeleton. As the Ambler moves along the push-off of K , he will pass through walls, or vertical 2-cells, whenever a strand K_r turns into a strand K_{r+1} , that is, at all lifts of crossings where an arc of K is the understrand. Passing through a wall at a lift of a positive crossing increases the superscript on the 3-cell by 1 (since a positively oriented meridian of the branching set acts on the 3-cells by the q -cycle $(123 \dots q)$). Similarly, passing through a wall at a lift of a negative crossing decreases the superscript of the 3-cell by 1. We introduce a function, $\omega_K(i)(j)$, to keep track of the positions of 3-cells: when the Ambler has the 1-cell k_i to his left, and he is standing on the 2-cell A_i^j , his head will be in the 3-cell $E^{\omega_K(i)(j)}$. Lastly, recall that we have arranged that the writhe of the knot is $0 \pmod q$. Therefore, if the Ambler starts a walk on a right push-off of k_0 , standing on A_0^j , after completing a full circle along a push-off of K , he has his head back in E^j , the 3-cell he started in.

It remains to label the lifts of the arcs η_i and of the 2-cells B_i . First observe that the pre-image of η in $\Sigma_q(K)$ has q path-lifts, which we label η^1, \dots, η^q . These path-lifts fit together to form

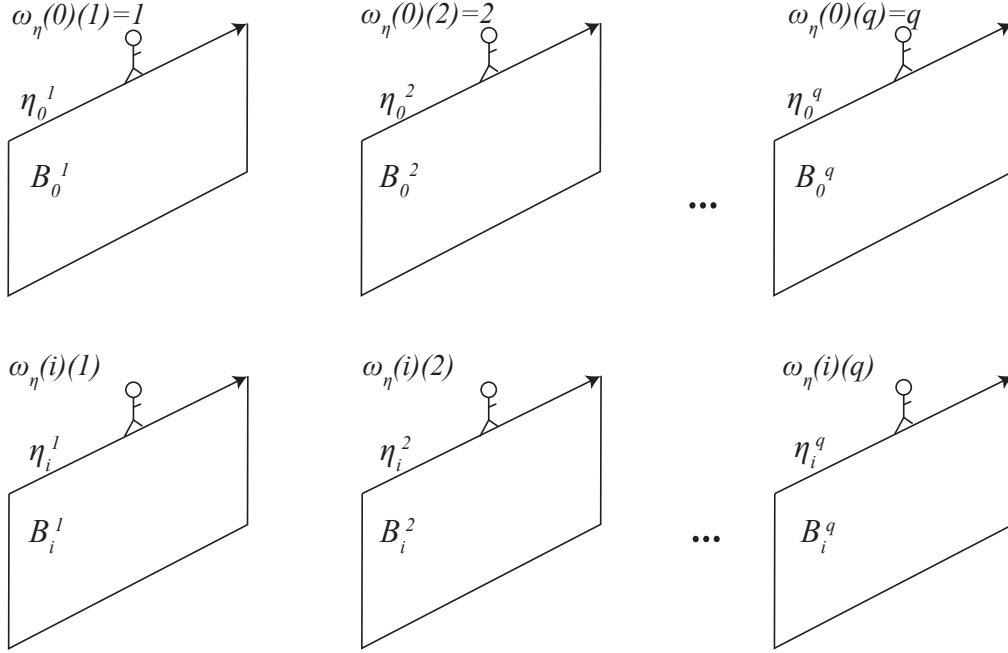


FIGURE 3. If the Ambler stands on the lift η_i^j of η_i above the 2-cell B_i^j , his head is in the 3-cell $E^{\omega_\eta(i)(j)}$. Since there are q lifts of each arc η_i , $\omega_\eta(i)$ is a permutation in the symmetric group S_q . We assume that $\omega_\eta(0)$ is the identity permutation.

closed, connected components. Recall that we refer to each such component as a pseudo-branch curve.

We next remark that $\forall i, j$ each component η^i contains a lift of the arc η_j , denoted η_j^i . This 1-cell bounds a 2-cell B_j^i , one of the lifts of B_j . We would like to have a systematic way of enumerating the components η^1, \dots, η^q . We choose the convention that the arc η_0^r is incident to the 3-cell E^r . That is, if the Ambler stands on B_0^r with η_0^r on his left, his head is in E^r . The component η^r is by definition the one containing the arc η_0^r .

The functions $\omega_\eta(i)(j)$ and $\omega_\gamma(i)(j)$ are defined similarly to $\omega_K(i)(j)$ above. In other words, assume the Ambler is standing on the arc η_i^j , above the 2-cell B_i^j . Then, his head is in $\omega_\eta(i)(j)$. See Figure 3.

We make one additional remark about the positions of 2-cell B_i . Recall we chose the convention that if the Ambler stands on η_0^k above B_0^k , his head is in E^k . Additionally, we assume B_i^k shares a (vertical) boundary 1-cell with B_{i+1}^k . In other words, if the Ambler is walking to the right of η along a push-off of η in the direction determined by the orientation of η , when he reaches a vertical wall, he crosses from B_i^k into B_{i+1}^k .

Now consider a crossing c_i in the given diagram of $K \cup \eta$, where the understrand k_i and the overstrand $k_{o(i)}$ are both arcs of the branching set K . The crossing has q lifts to $\Sigma_q(K)$ and the vertical 2-cells $A_{o(i)}^j$ are distributed across them. We introduce a function, $\sigma(i, j)$, to denote which lift of $A_{o(i)}$ lies over a given lift of A_i . Here, the subscript $o(i)$ denotes the overstrand at crossing i

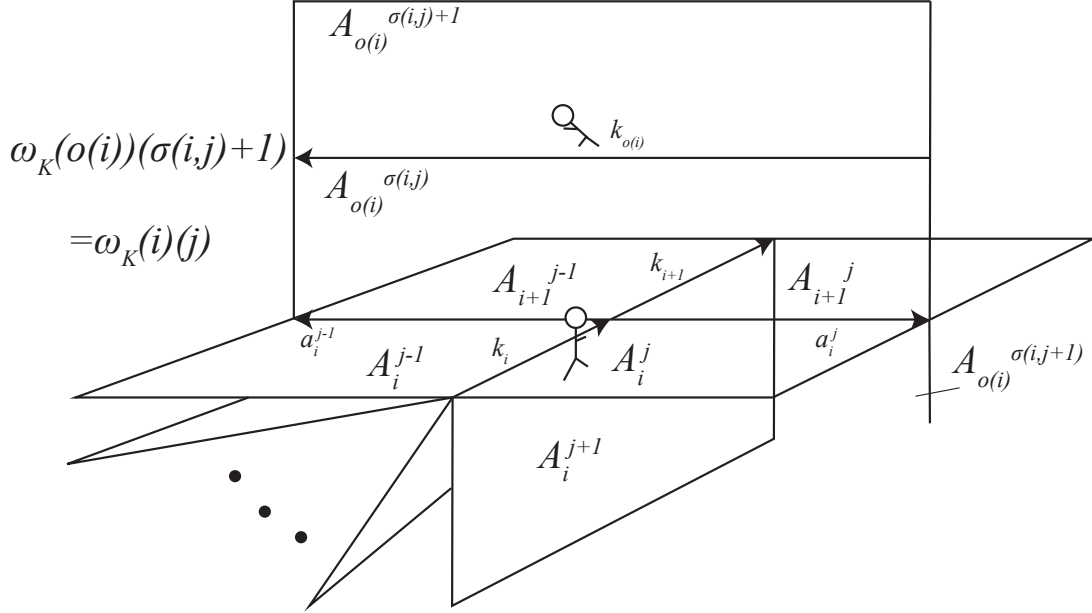
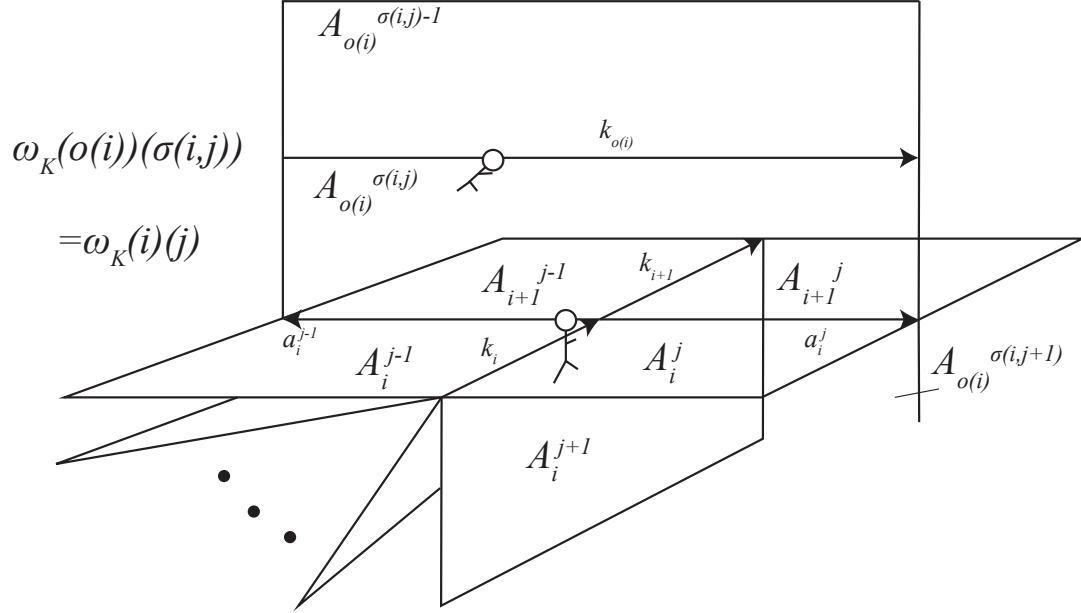


FIGURE 4. Lift of the cell structure at a positive (top) and negative (bottom) crossing of the branch curve K over the end of arc k_i , with Ambler.

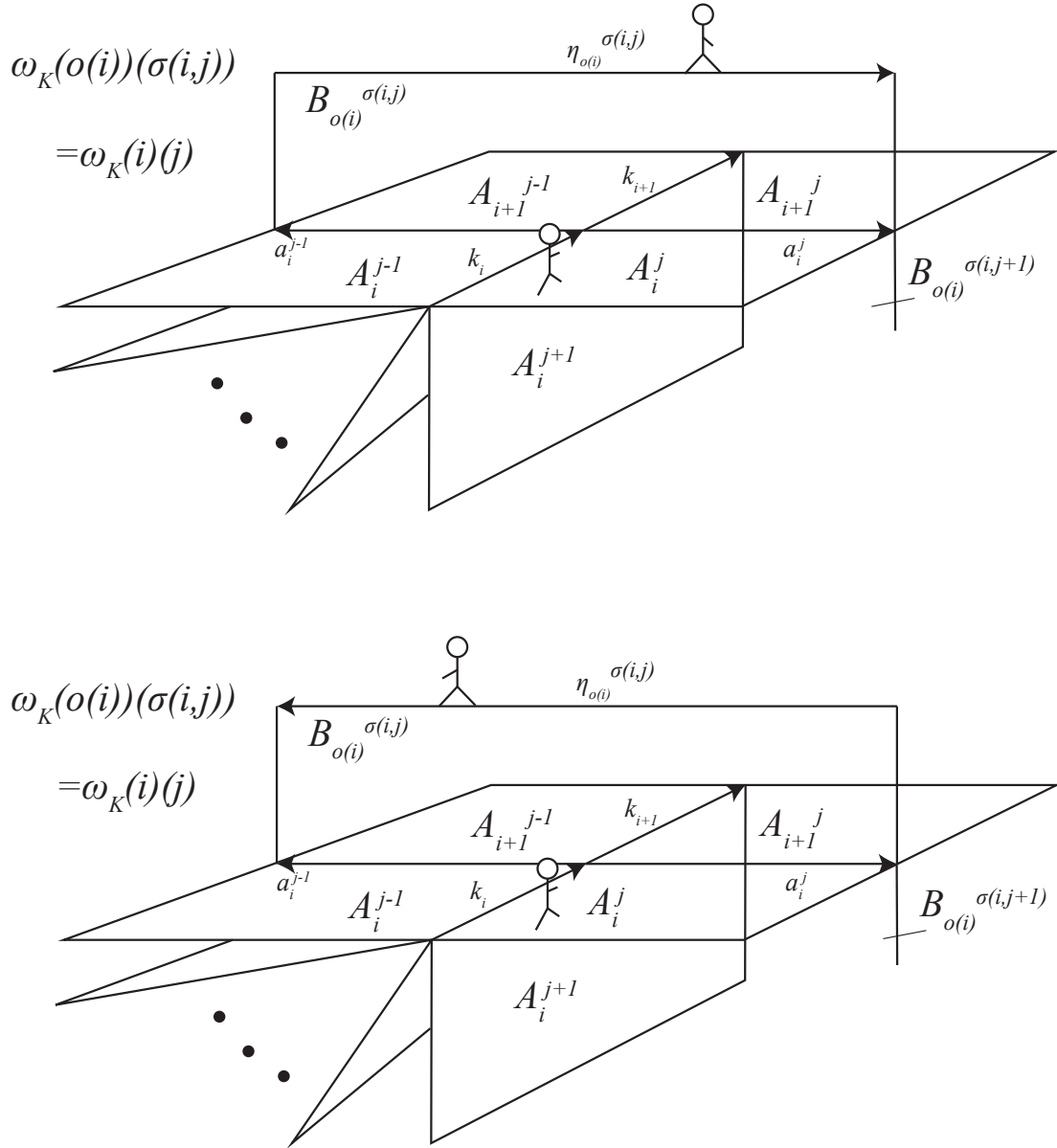


FIGURE 5. Lift of the cell structure at a positive (top) and negative (bottom) crossing of the pseudo-branch curve η over the end of arc k_i , with Ambler.

of the diagram. The superscript $\sigma(i, j)$ specifies which lift of the downstairs 2-cell $A_{o(i)}$ the Ambler will cross when passing from A_i^j to A_{i+1}^j in $\Sigma_q(K)$. Put yet another way, the 3-cells $E^{\omega_K(i)(j)}$ and $E^{\omega_K(i+1)(j)}$ share the 2-cell $A_{o(i)}^{\sigma(i,j)}$ as part of their boundary.

The case where the over-strand at the head of k_i is an arc of η is treated similarly. If the overstrand is $\eta_{o(i)}$, the relevant vertical wall in S^3 is $B_{o(i)}$ and its lifts $B_{o(i)}^{\sigma(i,j)}$ are labeled in the analogous fashion. That is, if the Ambler is standing on A_i^j with the knot on his left and walking in the direction of the orientation of the knot, the vertical wall he will cross when he reaches a lift of crossing i is $B_{o(i)}^{\sigma(i,j)}$.

We define a function $\sigma_\gamma(i, j)$ in the analogous fashion, to keep track of the superscripts of the vertical 2-cells the Ambler will cross when traveling along a lift of γ . Note that we do not define a function $\sigma_\eta(i, j)$ since, in computations, we never travel along η unless $\gamma = \eta$, as is the case in many applications. As a general principle, we do not name cells which do not come up in the computation. If interested in a 2-chain bounded by γ , and 2-cells intersected when traveling along a lift of η , we simply swap the roles of η and γ in the labeled diagram.

The values of the functions $\sigma(i, j)$ and $\sigma_\gamma(i, j)$ are determined by the following formulas.

Definition 1. The function $\sigma(i, j)$ is defined by:

$$\sigma(i, j) = \begin{cases} \omega_K(o(i))^{-1}[\omega_K(i)(j)] & \text{if } \epsilon(i) = 1 \text{ and } k_i \text{ terminates at the arc } k_{o(i)} \\ \omega_K(o(i))^{-1}[\omega_K(i)(j)] - 1 & \text{if } \epsilon(i) = -1 \text{ and } k_i \text{ terminates at the arc } k_{o(i)} \\ \omega_\eta(o(i))^{-1}[\omega_K(i)(j)] & \text{if } k_i \text{ terminates at the arc } \eta_{o(i)} \end{cases}$$

The output of $\sigma(i, j)$ is taken mod q with values between 1 and q .

Definition 2. The function $\sigma_\gamma(i, j)$ is defined by:

$$\sigma_\gamma(i, j) = \begin{cases} \omega_K(o_\gamma(i))^{-1}[\omega_\gamma(i)(j)] & \text{if } \epsilon_\gamma(i) = 1 \text{ and } \gamma_i \text{ terminates at the arc } k_{o_\gamma(i)} \\ \omega_K(o_\gamma(i))^{-1}[\omega_\gamma(i)(j)] - 1 & \text{if } \epsilon_\gamma(i) = -1 \text{ and } \gamma_i \text{ terminates at the arc } k_{o_\gamma(i)} \\ \omega_\eta(o(i))^{-1}[\omega_\gamma(i)(j)] & \text{if } \gamma_i \text{ terminates at the arc } \eta_{o_\gamma(i)} \end{cases}$$

The output of $\sigma_\gamma(i, j)$ is taken mod q with values between 1 and q .

The notation is summarized in Table 1.

3. MAIN THEOREM, SPECIALIZED VERSION

To simplify the exposition, we first tailor the theorem to our primary application. That is, we begin by assuming that each of η and γ have q closed lifts, η^1, \dots, η^q and $\gamma^1, \dots, \gamma^q$. This happens precisely when q divides the linking number of both η and γ with K . We give the general linking number formula, with no assumption on the linking numbers in S^3 , in Section 4.

Given a link $K \cup \eta \cup \gamma$ as above, for each lift η^k of η and γ^j of γ to $\Sigma_q(K)$, we check if there exists a rational two-chain with boundary η^k and γ^j , respectively. If such chains exist, we find an explicit formula for the chain bounding η^k and use it to compute the linking number of η^k with γ^j .

A priori, a (rational) 2-chain bounding η^k , the k^{th} lift of η , if it exists, takes the form

$$\Sigma^k = \sum_{i=0}^{m-1} z_i^k B_i^k + \sum_{i=0}^{n-1} x_i^j A_i^j.$$

K	branching set
q	degree of branched cover (in applications, $q = p^s$ for some prime p)
$\Sigma_q(K)$	q -fold cover of S^3 branched along K
η, γ	simple closed curves in $S^3 \setminus K$ (co-called pseudo-branch curves)
n	number of strands of K in diagram of $K \cup \eta$
k_i	strand of K and horizontal 1-cell in either S^3 or $\Sigma_q(K)$
η_i	strand of η and horizontal 1-cell in either S^3 or $\Sigma_q(K)$
a_i	vertical 1-cell in S^3 , at crossing i
$o(i)$	subscript of the overstrand at crossing i
$\epsilon(i) \in \{\pm 1\}$	sign of crossing at the head of the arc k_i
$\epsilon_\gamma(i) \in \{\pm 1\}$	sign of the crossing at the head of the arc γ_i
A_i	2-cell in S^3 with $\partial(A_i) = k_i + a_{i+1} - a_i$
A_i^1, \dots, A_i^q	lifts of A_i to $\Sigma_q(K)$, with indices increasing clockwise around K_i
$\eta^1, \eta^2, \dots, \eta^q$	closed components of the lift of η to $\Sigma_q(K)$
η_i^j	lift of the arc η_i contained in the component η^j
m	number of strands of η in diagram of $K \cup \eta$
B_i	2-cell whose horizontal boundary is η_i
B_i^1, \dots, B_i^q	lifts of B_i to $\Sigma_q(K)$, with B_i^k having η_i^k on its boundary
$\omega_K(i)$	permutation associated to arc K_i
$\omega_K(i)(x) = y$	when the Ambler stands on A_i^x with k_i on his left, his head is in E^y
$\omega_\eta(i)(j)$	3-cell containing the Ambler's head when he stands on the lift B_i^j of B_i
$\omega_\gamma(i)$	permutation of the 3-cells associated to arc γ_i , analogous to $\omega_\eta(i)$
$\sigma(i, j)$	superscript on the vertical wall ($A_{o(i)}^{\sigma(i,j)}$ or $B_{o(i)}^{\sigma(i,j)}$) separating A_i^j and A_{i+1}^j
$\sigma_\gamma(i, j)$	superscript on the vertical wall ($A_{o(i)}^{\sigma_\gamma(i,j)}$ or $B_{o(i)}^{\sigma_\gamma(i,j)}$) separating γ_i^j and γ_{i+1}^j
Σ^k	rational two-chain with boundary η^k
x_i^j	coefficient of A_i^j in a given 2-chain Σ^k

TABLE 1. Notation

The 1-cell η_i^k appears as a boundary of only one 2-cell, B_i^k . This implies that the coefficient of η_i^k in $\partial\Sigma^k$ is z_i^k . Since $\partial\Sigma^k = \eta^k = \sum_{i=0}^{m-1} \eta_i^k$, we have $z_i^k = 1$. Thus, we can rewrite the above chain as:

$$(1) \quad \Sigma^k = \sum_{i=0}^{m-1} B_i^k + \sum_{i=0}^{n-1} x_i^j A_i^j.$$

Additionally, for any arc k_i of K , the coefficient of k_i in $\partial\Sigma^k$ is $\sum_{j=1}^q x_i^j$. Since $\partial\Sigma^k = \eta^k$, we conclude that $\sum_{j=1}^q x_i^j = 0$ for each i .

The remaining constraints, a system of linear equations in the x_i^j , are summarized in Theorem 2.

Theorem 2. *Let $K \cup \eta$ be a link in S^3 . Let q be an integer dividing $lk(K, \eta)$. We use the notation of Section 2. The lift η^k of $\eta \in S^3(K)$ to $\Sigma_q(K)$, if rationally nullhomologous, bounds the 2-chain Σ^k in Equation 1, where the x_i^j satisfy $\sum_{j=1}^q x_i^j = 0$ for each i , and are simultaneously a solution*

to the following system:

$$\begin{cases} x_i^j - x_{i+1}^j - \epsilon(i)(x_{o(i)}^{\sigma(i,j)} - x_{o(i)}^{\sigma(i,j+1)}) = 0 & \text{if } k_i \text{ terminates at the arc } k_{o(i)} \\ x_i^j - x_{i+1}^j = \epsilon(i) & \text{if } k_i \text{ terminates at the arc } \eta_{o(i)} \text{ and } \sigma(i, j) = k \\ x_i^j - x_{i+1}^j = -\epsilon(i) & \text{if } k_i \text{ terminates at the arc } \eta_{o(i)} \text{ and } \sigma(i, j+1) = k \\ x_i^j - x_{i+1}^j = 0 & \text{if } k_i \text{ terminates at the arc } \eta_{o(i)} \text{ and } \sigma(i, j), \sigma(i, j+1) \neq k, \end{cases}$$

with superscripts taken mod q between 1 and q , and subscripts taken mod n between 0 and $n-1$. If the system of equations above has no solution over \mathbb{Q} , η^k is non-zero in $H_1(\Sigma_q; \mathbb{Q})$.

Proof. Suppose $\partial\Sigma^k = \eta^k$, with

$$\Sigma^k = \sum_{i=0}^{m-1} B_i^k + \sum_{i=0}^{n-1} x_i^j A_i^j.$$

Let i be the crossing where the arc k_i terminates. We compute the contribution to $\partial\Sigma^k$ by cells in the lift of a neighborhood of the crossing i to M , which we denote by $\partial|_i\Sigma^k$. (We will consider 4 different types of crossings, as in the theorem statement; the first case corresponds to the first crossing type, and the second case covers the other three crossing types.)

Case 1: At crossing i , k_i terminates at the arc $k_{o(i)}$. The cell structure in the lift of a neighborhood of a crossing i of this type is shown in Figure 4.

In this case, $\partial|_i\Sigma^k$ takes the form

$$\partial|_i\Sigma^k = \left(\sum_{j=1}^q x_i^j \right) k_i + \left(\sum_{j=1}^q x_{i+1}^j \right) k_{i+1} + \left(\sum_{j=1}^q x_{o(i)}^j \right) k_{o(i)} + \sum_{i=1}^q y_i^j \alpha_i^j,$$

where y_i^j is a linear combination of the x_r^s , determined by the configuration of cells at the given crossing. As previously established (see paragraph preceding the theorem statement), $\sum_{j=1}^q x_i^j = 0$, $\sum_{j=1}^q x_{i+1}^j = 0$, and $\sum_{j=1}^q x_{o(i)}^j = 0$. In addition, each linear combination y_i^j of the x_r^s 's is equal to 0, since y_i^j is the coefficient of α_i^j in $\partial\Sigma^k = \eta^k$.

We now express y_i^j in terms of the x_r^s . Refer again to Figure 4, where both cases, $\epsilon(i) = 1$ and $\epsilon(i) = -1$, are depicted.

First suppose $\epsilon(i) = 1$. In this case, α_i^j is incident to A_i^j , A_{i+1}^j , $A_{o(i)}^{\sigma(i,j)}$, and $A_{o(i)}^{\sigma(i,j+1)}$, and appears in the boundaries of these 2-cells with coefficients x_i^j , $-x_{i+1}^j$, $-x_{o(i)}^{\sigma(i,j)}$, and $x_{o(i)}^{\sigma(i,j+1)}$. Therefore, $y_i^j = x_i^j - x_{i+1}^j - x_{o(i)}^{\sigma(i,j)} + x_{o(i)}^{\sigma(i,j+1)}$.

The case $\epsilon(i) = -1$ is analogous, and we conclude that $y_i^j = x_i^j - x_{i+1}^j + x_{o(i)}^{\sigma(i,j)} - x_{o(i)}^{\sigma(i,j+1)}$.

Setting $y_i^j = 0$ in both cases above results in the equation

$$x_i^j - x_{i+1}^j - \epsilon(i)(x_{o(i)}^{\sigma(i,j)} - x_{o(i)}^{\sigma(i,j+1)}) = 0,$$

which is the first equation in the theorem statement, as desired.

Case 2: At crossing i , k_i terminates at the arc $\eta_{o(i)}$. The cell structure in the lift of a neighborhood of a crossing i of this type is shown in Figure 5.

In this case,

$$\partial|_i \Sigma^k = \left(\sum_{j=1}^q x_i^j \right) k_i + \left(\sum_{j=1}^q x_{i+1}^j \right) k_{i+1} + \eta_{o(i)}^k + \sum_{i=1}^q y_i^j a_i^j,$$

where again y_i^j is a linear combination of the x_r^s . As in Case 1, the first two sums are zero, and each linear combination y_i^j of the x_r^s 's is equal to 0.

We again express y_i^j in terms of the x_r^s and set the result equal to 0 to obtain the desired linear equations.

The case $\epsilon(i) = 1$ is shown in the top of Figure 5. The only 2-cell of type B appearing at crossing i is $B_{o(i)}^k$. We observe that a_i^j is incident to A_i^j , A_{i+1}^j , $B_{o(i)}^{\sigma(i,j)}$, and $B_{o(i)}^{\sigma(i,j)}(i, j+1)$, and appears in the boundaries of these 2-cells with coefficients 1, -1, -1, and 1, respectively. If $\sigma(i, j) = k$, then $y_i^j = x_i^j - x_{i+1}^j - 1$. If $\sigma(i, j+1) = k$, then $y_i^j = x_i^j - x_{i+1}^j + 1$. Otherwise, $y_i^j = x_i^j - x_{i+1}^j$.

The case $\epsilon(i) = -1$ is similar, and shown in the bottom of Figure 5. In this case, a_i^j appears in the boundaries of A_i^j , A_{i+1}^j , $B_{o(i)}^{\sigma(i,j)}$, and $B_{o(i)}^{\sigma(i,j)}(i, j+1)$ with coefficients 1, -1, 1, and -1 respectively. If $\sigma(i, j) = k$, then $y_i^j = x_i^j - x_{i+1}^j + 1$. If $\sigma(i, j+1) = k$, then $y_i^j = x_i^j - x_{i+1}^j - 1$. Otherwise, $y_i^j = x_i^j - x_{i+1}^j$.

Putting these two cases $\epsilon(i) = \pm 1$ together, and setting $y_i^j = 0$, we get the final three equations

$$\begin{cases} x_i^j - x_{i+1}^j = \epsilon(i) & \text{if } k_i \text{ terminates at the arc } \eta_{o(i)} \text{ and } \sigma(i, j) = k \\ x_i^j - x_{i+1}^j = -\epsilon(i) & \text{if } k_i \text{ terminates at the arc } \eta_{o(i)} \text{ and } \sigma(i, j+1) = k \\ x_i^j - x_{i+1}^j = 0 & \text{if } k_i \text{ terminates at the arc } \eta_{o(i)} \text{ and } \sigma(i, j), \sigma(i, j+1) \neq k, \end{cases}$$

as desired. □

Theorem 3. *Let $K \cup \eta \cup \gamma$ be a link in S^3 . We adopt the notation and hypotheses of Theorem 2, and in particular assume that q divides the linking numbers of η and γ with K . In addition, if $\gamma = \eta$, we assume in what follows that $j \neq k$. If γ^j and η^k are rationally null-homologous in $\Sigma_q(K)$, the linking number of the lift γ^j with the lift η^k , with $\eta^k = \partial \Sigma^k$ defined as in Theorem 2 is $\text{lk}(\gamma^j, \eta^k) = \sum_{i=0}^{s-1} a_i$, where*

$$(2) \quad a_i = \begin{cases} \epsilon_\gamma(i) \cdot x_{o_\gamma(i)}^{\sigma_\gamma(i,j)} & \text{if } \gamma_i \text{ terminates at the arc } k_{o_\gamma(i)} \\ \epsilon_\gamma(i) & \text{if } \gamma_i \text{ terminates at the arc } \eta_{o_\gamma(i)} \text{ and } \sigma_\gamma(i, j) = k \\ 0 & \text{otherwise} \end{cases}$$

Proof. Recall that, if η^k bounds the rational chain Σ^k , the linking number $\text{lk}(\gamma^j, \eta^k)$ equals the signed intersection number between γ^j and Σ^k . This number is symmetric and independent of the choice of two-chain [3]. To compute the intersection number, we first need to ensure that γ^j and Σ^k are transverse. Recall that we started with a generic projection of the link diagram and we obtained the 2-skeleton by taking the cone on $K \cup \eta$; we then lifted this cell structure to $\Sigma_q(K)$. Therefore, by construction, γ^j , a lift of γ , is transverse to all 2-cells in $\Sigma_q(K)$ except (in the case

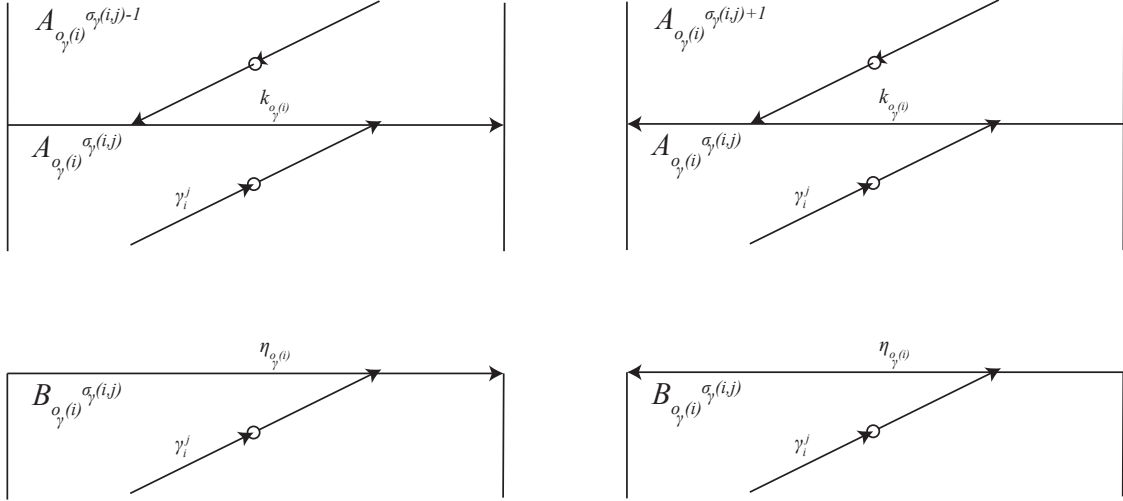


FIGURE 6. The lift second pseudo-branch curve γ and the cell structure when γ_i terminates at an arc of the knot K (top, positive and negative crossings) and at an arc of the first pseudo-branch curve η (bottom, positive and negative crossings).

where $\gamma = \eta$) those it bounds. By assumption, $\gamma^j \neq \eta^k$ and therefore, by Equation 1, γ^j is not on the boundary of any of the 2-cells in Σ^k . In sum, γ^j is transverse to all cells in the 2-chain Σ^k .

Recall that γ^j can be regarded as a boundary union of embedded arcs, $\gamma^j = \sum_{i=0}^{s-1} \gamma_i^j$. These endpoints are lifts of crossings in the diagram where γ passes under K or η . Moreover, intersections between γ^j and Σ^k can only occur at the endpoints of these arcs.

For each pair i, j , we consider endpoint where the arc γ_i^j terminates. Which type (A or B) of vertical 2-cell this endpoint belongs to is determined by the link component (K or η , respectively) containing the over-strand at the crossing where the i -th strand of γ ends. The subscript of the 2-cell is determined by the function $o_\gamma(i)$, and the superscript by the function $\sigma_\gamma(i, j)$. The coefficient of this 2-cell in Σ^k equals $x_{o_\gamma(i)}^{\sigma_\gamma(i, j)}$ if it is an A cell; 1 if it is a B cell with horizontal boundary belonging to η^k ; 0 otherwise. (The reader may refer again to Equation 1.) Finally, the sign of the intersection between the 2-cell and γ^j is determined by the function $\epsilon_\gamma(i)$. The term a_i in the theorem statement is computed from the above data: it equals 0 if the 2-cell where γ_i^j terminates is not part of Σ^k ; otherwise it equals the coefficient of this 2-cell times the sign of the crossing. \square

4. MAIN THEOREM, GENERAL CASE

We now drop the hypothesis that q divides the linking numbers $\text{lk}(K, \eta)$ and $\text{lk}(K, \gamma)$.

As before, η (respectively γ) has q path-lifts, η^1, \dots, η^q , labeled so that η_0^k is in the 3-cell E^k ; but the η^k may not be closed loops. However, the η^i fit together to form closed components, what we call pseudo-branch curves, and we can compute linking numbers between these closed components and the corresponding closed components for γ .

First, observe that the number, I_η , of connected components in the lift of η equals the index, in $\mathbb{Z}/q\mathbb{Z}$, of the subgroup generated by $\text{lk}(K, \eta)$. Traveling along a component of the lift of η , one will encounter path-lifts η^r, η^s, \dots whose indices jump by $\text{lk}(K, \eta) \bmod q =: \bar{l}_\eta$, until they begin

to repeat. The pseudo-branch curves $\boldsymbol{\eta}^k$ projecting to η are therefore

$$\boldsymbol{\eta}^k = \eta^k \cup \eta^{k+\bar{l}_\eta} \cup \dots \cup \eta^{k+(q/I-1)\cdot\bar{l}_\eta},$$

where $k \in \{1, \dots, I_\eta\}$. The superscripts correspond to elements of the coset $G_\eta^k = k + \langle \bar{l}_\eta \rangle$ in $\mathbb{Z}/q\mathbb{Z}$, with values taken in $\{1, \dots, q\}$. We define the closed component $\boldsymbol{\gamma}^j$ as well as G_γ^j analogously, with $j \in \{1, \dots, I_\gamma\}$.

Reasoning as we did in order to arrive at Equation 1, we see that a generic 2-chain bounding $\boldsymbol{\eta}^k$, if it exists, takes the form

$$(3) \quad \Sigma^k = \sum_{k' \in G_\eta^k} \left(\sum_{i=0}^{m-1} B_i^{k'} \right) + \sum_{i=0}^{n-1} x_i^j A_i^j.$$

Theorem 4. *Let $K \cup \eta$ be a link in S^3 . We use the notation of Section 2. The pseudo-branch component $\boldsymbol{\eta}^k$ of $\eta \in S^3(K)$ in $\Sigma_q(K)$, if rationally nullhomologous, bounds the 2-chain Σ^k in Equation 3, where the x_i^j satisfy $\sum_{j=1}^q x_i^j = 0$ for each i , and are simultaneously a solution to the following system:*

$$\left\{ \begin{array}{ll} x_i^j - x_{i+1}^j - \epsilon(i)(x_{o(i)}^{\sigma(i,j)} - x_{o(i)}^{\sigma(i,j+1)}) = 0 & \text{if } k_i \text{ terminates at the arc } k_{o(i)} \\ x_i^j - x_{i+1}^j = \epsilon(i) & \text{if } k_i \text{ terminates at the arc } \eta_{o(i)}, \\ & \sigma(i,j) \in G_\eta^k, \text{ and } \sigma(i,j+1) \notin G_\eta^k \\ x_i^j - x_{i+1}^j = -\epsilon(i) & \text{if } k_i \text{ terminates at the arc } \eta_{o(i)}, \\ & \sigma(i,j+1) \in G_\eta^k, \text{ and } \sigma(i,j) \notin G_\eta^k \\ x_i^j - x_{i+1}^j = 0 & \text{if } k_i \text{ terminates at the arc } \eta_{o(i)} \text{ and} \\ & \{\sigma(i,j), \sigma(i,j+1)\} \subset G_\eta^k \text{ or } \{\sigma(i,j), \sigma(i,j+1)\} \cap G_\eta^k = \emptyset \end{array} \right.$$

with superscripts taken mod q between 1 and q , and subscripts taken mod n between 0 and $n-1$. If the system of equations above has no solution over \mathbb{Q} , $\boldsymbol{\eta}^k$ is non-zero in $H_1(\Sigma_q; \mathbb{Q})$.

The proof of Theorem 4 is analogous to the proof of Theorem 2 but this time taking into account the way different path lifts combine to form connected components.

Now to compute the linking number of $\boldsymbol{\gamma}^j$ with $\boldsymbol{\eta}^k$, we first use Theorem 4 to find a rational 2-chain Σ^k bounding $\boldsymbol{\eta}^k$, and to verify that $\boldsymbol{\gamma}^j$ is rationally null-homologous. We then determine the linking numbers according to the following formula:

Theorem 5. *Let $K \cup \eta \cup \gamma$ be a link in S^3 . We adopt the notation and hypotheses of Theorem 4. In addition, if $\gamma = \eta$, we assume in what follows that $j \neq k$. If $\boldsymbol{\gamma}^j$ and $\boldsymbol{\eta}^k$ are rationally null-homologous in $\Sigma_q(K)$, the linking number of the lift $\boldsymbol{\gamma}^j$ with the lift $\boldsymbol{\eta}^k$, with $\boldsymbol{\eta}^k = \partial \Sigma^k$ defined as in Theorem 4 is $lk(\boldsymbol{\gamma}^j, \boldsymbol{\eta}^k) = \sum_{j' \in G_\gamma^j} \left(\sum_{i=0}^{s-1} a_{i,j'} \right)$, where*

$$(4) \quad a_{i,j'} = \begin{cases} \epsilon_\gamma(i) \cdot x_{o_\gamma(i)}^{\sigma_\gamma(i,j')} & \text{if } \gamma_i \text{ terminates at the arc } k_{o_\gamma(i)} \\ \epsilon_\gamma(i) & \text{if } \gamma_i \text{ terminates at the arc } \eta_{o_\gamma(i)} \text{ and } \sigma_\gamma(i,j') \in G_\eta^k \\ 0 & \text{otherwise} \end{cases}$$

The proof of Theorem 5 is analogous to the proof of Theorem 3. The contribution of each intersection point of a path-lift of γ and a 2-cell in Σ^k is computed as before; these contributions are then distributed across connected components $\boldsymbol{\gamma}^j$ as dictated by the indexing sets G_γ^j .

5. APPLICATIONS

One application of computing linking numbers of pseudobranch curves in cyclic branched covers is to obstruct satellite operations from inducing homomorphisms on concordance, using the following results from [14]. Throughout this section, η denotes a meridian of the solid torus in which the satellite pattern is embedded.

Theorem 6. [14] *Let P be a pattern in the solid torus with winding number w , and let q be a prime power dividing w . Suppose that the lifts η_1, \dots, η_q of η to $\Sigma_q(P(U))$ are null-homologous in $\Sigma_q(P(U))$. If $lk(\eta_i, \eta_j) \geq 0$ for all $i \neq j$, but is not identically zero, then P does not induce a homomorphism of the smooth concordance group.*

Theorem 7. [14] *Let P be a pattern in the solid torus with winding number w , and let q be a prime power dividing w . Let η_1, \dots, η_q denote the lifts of η to $\Sigma_q(P(U))$ and let n denote the order of $[\eta_1]$ in $H_1(\Sigma_q(P(U)))$. Suppose that either n is odd or w is a nonzero multiple of n . If $lk(\eta_i, \eta_j) \geq 0$ for all $i \neq j$, but is not identically zero, then P does not induce a homomorphism of the smooth concordance group.*

In this section, we apply our theorem to evaluate, in a variety of cases, the above obstructions. To start, we recover the (easy) fact that for $n \neq \pm 1$ the $(n, 1)$ cable map does not induce a homomorphism on smooth concordance. In Example 1, we also consider certain satellites obtained by crossing changes in the standard diagram of the cabling pattern. We include these examples in part because the results are verifiable by hand (contrast Example 3), since the branching set, $P(U)$, is an unknot. In addition, these computations lead to the observation (Corollary 9) that for any knot $K \subset S^3$ there are infinitely many embeddings of K in the solid torus, of arbitrarily large winding numbers, that produce patterns for which the homomorphism obstruction in Theorem 6 vanishes. Next, in Example 2, we show that a family of satellite patterns determined by the Stevedore knot (embedded in different ways in a solid torus) do not induce homomorphisms on smooth concordance. We conclude with Example 3, which serves to illustrate that our method can handle knots of large Seifert genus, as well as high degree covers, without sweat.

Example 1. We consider the $(n, 1)$ cabling operation, as well as satellites obtained by crossing changes in the standard diagrams for those cables. The point here is to give explicit and relatively easily visualizable two-chains for the lifts of η , in a family of examples where the answer can also be obtained by a geometric argument. (Compare Example 1.3 of [14].)

First consider the diagram for the $(n, 1)$ cable, together with a choice of η , shown in Figure 7 in the case $n = 5$. We will construct the 2-chain Σ^1 bounded by η^1 . The 2-chains bounding the other lifts of η can be obtained by acting on the superscripts of the coefficients of the cells in Σ^1 by a cyclic permutation. For each arc k_i in the diagram, we give a vector whose entries are the coefficients $(x_i^1, x_i^2, \dots, x_i^q)$ of the 2-cells $A_i^1, A_i^2, \dots, A_i^q$ in the 2-chain Σ^1 . Letting e_j denote the usual standard basis vector in \mathbb{Q}^q with a 1 in position j and 0's elsewhere, we have

$$(5) \quad (x_i^1, x_i^2, \dots, x_i^q) = \begin{cases} e_{n-i/2} - e_1 & \text{if } i \text{ even} \\ e_{n-(i-1)/2} - e_1 & \text{if } i \text{ odd} \end{cases}$$

These vectors, together with their corresponding arcs k_i of the cable diagram, are shown in Figure 7. Lastly, Σ^1 also contains each B_i^1 , per Equation 1. The 2-cells in the 2-chain described above are pictured, shaded, in Figure 8.

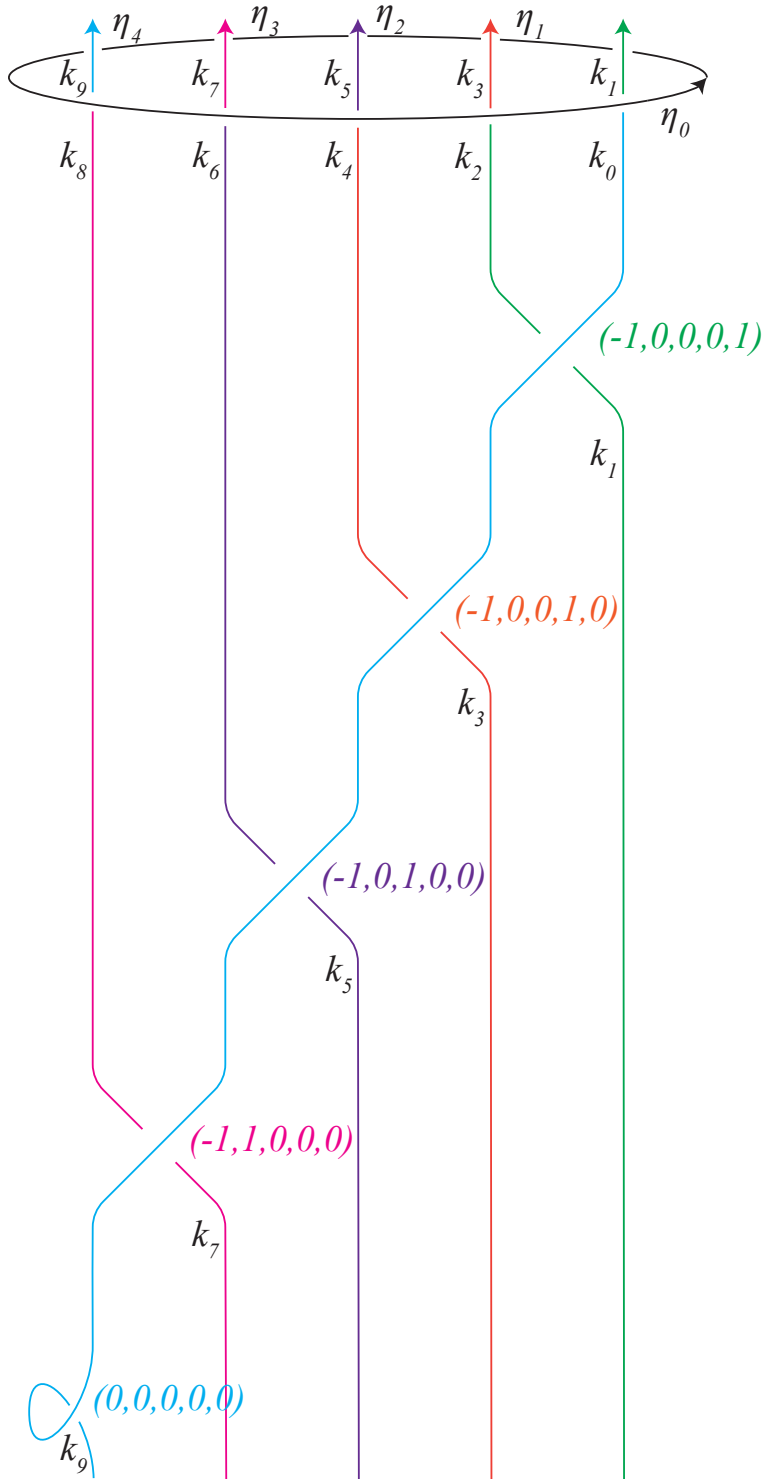


FIGURE 7. A numbered diagram of the $(5, 1)$ -cable, illustrating Equation 5 for the case $n = 5$. For each arc k_i of the cable, the vector of the same color lists the coefficients $(x_i^1, x_i^2, x_i^3, x_i^4, x_i^5)$ of the 2-cells A_i^1, \dots, A_i^5 that appear in the 2-chain bounding η_1 .

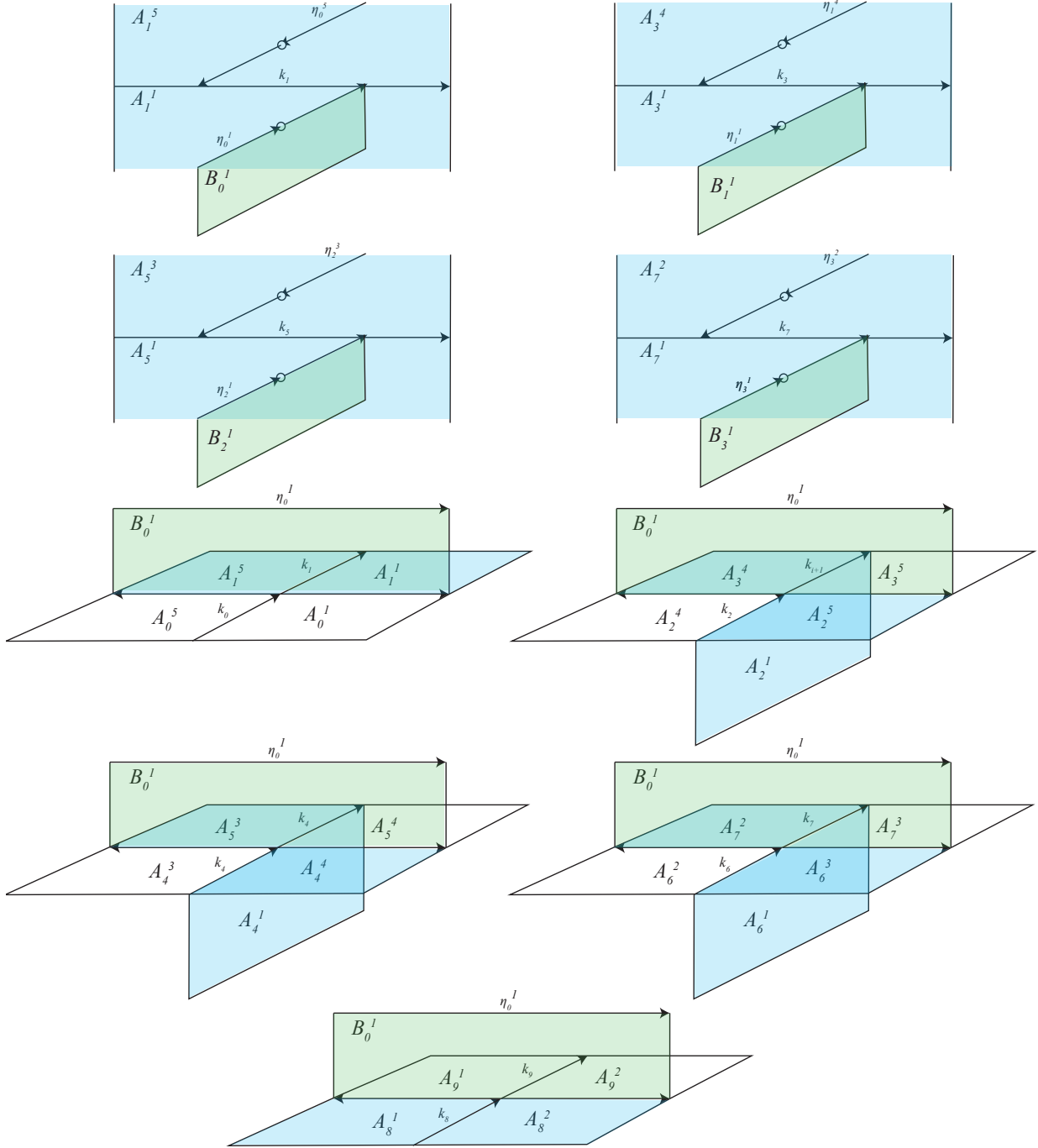


FIGURE 8. The blue and green 2-cells appear in a 2-chain bounding the lift η^1 of the pseudo-branch curve η for the $(5, 1)$ -cable, corresponding to the numbered diagram in Figure 7.

To compute the linking number of the lift η^k ($k \neq 1$) with η^1 , we count signed intersections of η^k with the 2-cells in Σ^1 . Observe in Figure 8 for the case $n = 5$ (an analogous picture can be drawn for the general case) that the only arc η_i^k that terminates at a cell of Σ^1 is η_{n-k}^k . Furthermore,

k	Lift η^i	Coefficients of 2-Chain for η^i $(x_0^1, x_0^2, x_0^3 x_1^1, x_1^2, x_1^3 x_2^1, x_2^2, x_2^3 x_3^1, x_3^2, x_3^3 x_4^1, x_4^2, x_4^3 x_5^1, x_5^2, x_5^3)$	$\text{lk}(\eta^1, \eta^i)$
0	η^1	$(0, 0, 0 -1, 0, 1 -1, 0, 1 -1, 1, 0 0, 0, 0)$	0
0	η^2	$(0, 0, 0 1, -1, 0 1, -1, 0 0, -1, 1 0, -1, 1 0, 0, 0)$	1
0	η^3	$(0, 0, 0 0, 1, -1 0, 1, -1 1, 0, -1 1, 0, -1 0, 0, 0)$	1
1	η^1	$(0, 0, 0 -1, 2, -1 0, 1, -1 1, 0, -1 1, 0, -1 0, 0, 0)$	0
1	η^2	$(0, 0, 0 -1, -1, 2 -1, 0, 1 -1, 1, 0 -1, 1, 0 0, 0, 0)$	0
1	η^3	$(0, 0, 0 2, -1, -1 1, -1, 0 0, -1, 1 0, -1, 1 0, 0, 0)$	0
2	η^1	$(0, 0, 0 -2, 1, 1 0, -3, 3 0, -2, 2 0, -1, 1 0, 0, 0)$	0
2	η^2	$(0, 0, 0 1, -2, 1 3, 0, -3 2, 0, -2 1, 0, -1 0, 0, 0)$	-1
2	η^3	$(0, 0, 0 1, 1, -2 -3, 3, 0 -2, 2, 0 -1, 1, 0 0, 0, 0)$	-1

TABLE 2. Outline of linking number computation for patterns obtained from the standard diagram of the $(3, 1)$ cable by changing the k rightmost crossings. Refer to Table 1 for the 2-cells whose coefficients are given by the x_i^j . The numbering of the arcs k_i corresponding to these coefficients is analogous to that of Figure 7, with the arc k_0 in the lower left.

the arc η_{n-k}^k terminates at the cell $A_{2(n-k)+1}^k$, which according to Equation 5 appears in Σ^1 with coefficient $+1$. Therefore the linking number $\text{lk}(\eta^k, \eta^1)$ is equal to 1.

See Table 2 to get a sense for how the 2-chains vary for other satellites obtained from the cable by k crossing changes in the case $n = 3$. See Table 3 to get a sense of how the linking numbers change for larger n and k .

In particular, the fact that the linking numbers of the lifts of η for the alternating cables are 0 can be deduced by similar reasoning as applied to the standard $(n, 1)$ cable above. We omit this technical argument in favor of the geometric one given below.

It is implicit in [15, 14] that alternating cabling patterns do not induce homomorphisms on concordance, and also that the linking number obstruction vanishes for these patterns. Indeed, if $P(U)$ is isotopic to $-P(U)$ inside $S^1 \times D^2$, then the linking numbers between lifts of η to a cyclic branched cover of $P(U)$ must be zero: on the one hand, mirroring changes the sign of these linking numbers (while the choice of orientation on the branching set leaves the numbers unchanged); on the other hand, the pattern is isotopic to its inverse. In other words, the homomorphism obstruction vanishes for patterns which are amphichiral inside the solid torus. This property is not affected by introducing local knotting, as we now recall.

The following is well known.

Lemma 8. *Let $K \subset S^3$ be a knot and $\eta, \gamma \subset S^3 \setminus K$ two disjoint simple closed curves. Let S be a 2-sphere embedded in S^3 so that the Heegaard splitting determined by S , $S^3 = B_1^3 \cup_S B_2^3$, has the property that $B_2^3 \cap K$ is an unknotted arc ξ properly embedded in B_2^3 ; and B_1^3 contains both η and γ in its interior. The linking numbers between lifts of η and γ to $\Sigma_q(K)$ are not affected by local knotting of ξ . Put differently, if a connected sum $K \# J$ is formed by replacing ξ with a knotted 1-tangle, the linking numbers between lifts of η and γ to $\Sigma_q(K)$ are equal to the linking numbers between the corresponding lifts to $\Sigma_q(K \# J)$.*

n	k	$\text{lk}(\eta^1, \eta^2), \text{lk}(\eta^1, \eta^3), \dots, \text{lk}(\eta^1, \eta^n)$
3	0	1, 1
3	1	0, 0
3	2	-1, -1
5	0	1, 1, 1, 1
5	1	0, 1, 1, 0
5	2	0, 0, 0, 0
5	3	0, -1, -1, 0
5	4	-1, -1, -1, -1
7	0	1, 1, 1, 1, 1, 1
7	1	0, 1, 1, 1, 1, 0
7	2	0, 0, 1, 1, 0, 0
7	3	0, 0, 0, 0, 0, 0
7	4	0, 0, -1, -1, 0, 0
7	5	0, -1, -1, -1, -1, 0
7	6	-1, -1, -1, -1, -1, -1

TABLE 3. Linking numbers for the pattern $C_{n,k}$ obtained from the $(n, 1)$ cable by k crossing changes.

Proof. We first note that the linking numbers of both η and γ with K are not changed by local knotting of ξ inside B_2^3 , so the preimage of η (resp. γ) has the same number of components in $\Sigma_q(K)$ as in $\Sigma_q(K\#J)$ and there is a natural identification between the components in the two covers.

The q -fold cyclic cover of B_2^3 branched along the trivial 1-tangle ξ is also a 3-ball, denoted \widehat{B}_2^3 . The q -fold cyclic cover $\Sigma_q(K\#J)$ can be obtained from $\Sigma_q(K)$ by replacing the interior of \widehat{B}_2^3 with a punctured copy of $\Sigma_q(J)$.

Now let η^k, γ^j be two connected components of the pre-images of η and γ , respectively, in $\Sigma_q(K)$. Since η, γ are disjoint from B_2^3 , we know that $(\eta^k \cup \gamma^j) \cap \widehat{B}_2^3 = \emptyset$. By a Meyer-Vietoris argument, η^k or γ^j are rationally nullhomologous in $\Sigma_q(K)$ if and only if they are so in $\Sigma_q(K\#J)$. Thus, the linking number is defined in $\Sigma_q(K)$ if and only if it's defined in $\Sigma_q(K\#J)$. Assume that this is the case. Then, some integer multiple of η^k bounds a 2-chain N in $\Sigma_q(K)$. This 2-chain can be assumed disjoint from \widehat{B}_2^3 and therefore can be used to compute the linking number between η^k and γ^j in $\Sigma_q(K\#J)$. \square

Corollary 9. *Let $K \subset S^3$ be a knot and $q > 2$ a prime. K admits an embedding in $S^1 \times D^2$ of winding number q with the property that, for the satellite pattern P determined by this embedding, the linking numbers between the lifts of η to $\Sigma_q(K)$ are all 0. In particular, the obstruction from [14] can not be used to show that the pattern P does not induce a homomorphism on smooth concordance.*

Of course, if K is not slice, no satellite operation with $P(U) = K$ will induce a homomorphism on concordance.

Proof. Let P' a pattern be an alternating cable of winding number q . Since P' is isotopic in $S^1 \times D^2$ to its mirror, the linking number obstruction vanishes for P' . By Lemma 8, introducing K as a local knot in $P'(U)$ does not affect the value of the obstruction. This produces the desired embedding of K into the solid torus. \square

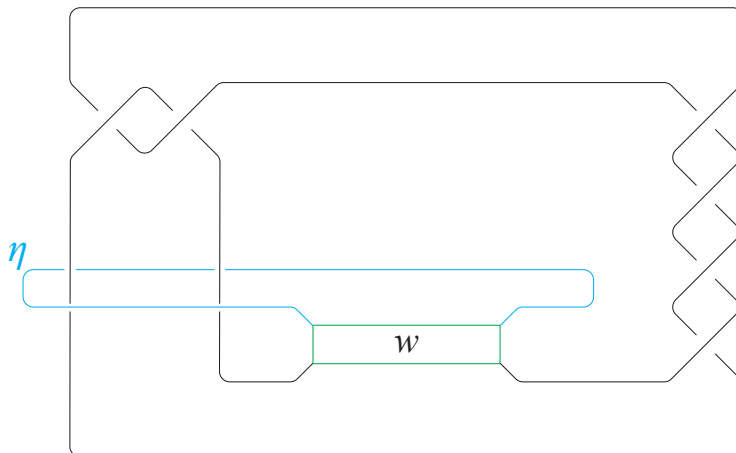


FIGURE 9. A family of patterns with increasing winding number, each with underlying knot the Stevedore knot. The box contains w full twists, ensuring that the winding number of the pattern in the solid torus is w .

On the other hand, the computations we did on the side, only a small number of which are included here, convinced us that that the homomorphism obstruction rarely vanishes. Next, we give one family of (slice) examples for which the relevant linking numbers take non-zero values.

Example 2. We consider several embeddings, of increasing winding number, of the Stevedore knot into the solid torus, and we show that the satellite operations determined by the resulting patterns do not induce homomorphisms on concordance. The linking numbers between the lifts of η are given in Table 4. We remark that the lifts of η in this example are not nullhomologous over \mathbb{Z} so we appeal to Theorem 7. We compute the linking numbers between lifts of η in the 2, 3, 4 and 5- fold covers of K , just to illustrate that it is easy, even though linking numbers in the 2-fold covers suffice to obstruct the pattern from inducing a homomorphism on concordance. Note that, in each case, an odd multiple of each η_i bounds, so its order in homology is odd, as required in the hypotheses of Theorem 7. Consequently, the order of the lift of each η_i is odd as well, so we can apply the Theorem.

To conclude, we compute the obstruction in a couple of cases where, in our estimate, the classical methods of [2] would be exceedingly challenging to use in practice, at least by hand (and we are not aware of any implementation of the technique). The patterns here are determined by two-bridge slice knots whose Seifert genus grows. For these examples, we also perform the computation for high degree covers, i.e. for relatively large values of q .

Example 3. The 2-bridge knots $C(a_1, a_2, \dots, a_n, x, x+2, a_n, \dots, a_2, a_1)$ in the notation of [13] are ribbon. In this example, we set $a_i = 2$ for all i , $x = 2$, and $n = 2m$. We obtain a family of satellite patterns P_m by embedding each of these knots knot in the solid torus in the manner indicated in Figure 10 for the case $m = 2$. Since all twist parameters are even, the Seifert genus of the knot P_m is $m + 1$. The linking numbers of the lifts of η for the first few values of m are shown in Table 5. Note that, while we don't compute the order in homology of the curves η_i precisely, we verify that this order is odd as it divides an odd number in each case. Based on our computations, a sampling

Degree of cover q	Winding number w	Multiple of η_1 which bounds in $\Sigma_q(K)$	$\text{lk}(\eta^1, \eta^2), \text{lk}(\eta^1, \eta^3), \dots, \text{lk}(\eta^1, \eta^q)$
2	0	9	2/9
2	2	9	-7/9
2	4	9	-16/9
2	6	9	-25/9
2	8	9	-34/9
<hr/>			
3	0	7	1/7, 1/7
3	3	7	-6/7, -6/7
3	6	7	-13/7, -13/7
3	9	7	-20/7, -20/7
3	12	7	-27/7, -27/7
<hr/>			
4	0	45	1/9, 4/45, 1/9
4	4	45	-8/9, -41/45, -8/9
4	8	45	-17/9, -86/45, -17/9
4	12	45	-26/9, -131/45, -26/9
4	16	45	-35/9, -176/45, -35/9
<hr/>			
5	0	31	3/31, 2/31, 2/31, 3/31
5	5	31	-28/31, -29/31, -29/31, -28/31
5	10	31	-59/31, -60/31, -60/31, -59/31
5	15	31	-90/31, -91/31, -91/31, -90/31
5	20	31	-121/31, -122/31, -122/31, -121/31

TABLE 4. Linking numbers for Example 2: Stevedore patterns with increasing winding number w . See Figure 9.

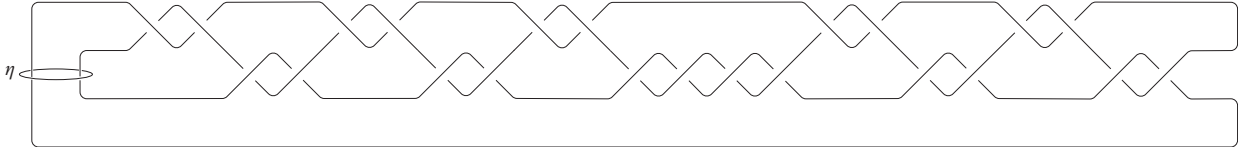


FIGURE 10. The pattern P_2 in the family of slice patterns P_m with winding number 0.

of which is included in Table 5, we would be surprised if linking numbers failed to obstruct any of the patterns P_m from inducing homomorphisms on concordance, using Theorem 7.

We invite the reader to test any pattern they are interested in, using the code provided in [5] and the instructions given in the Appendix.

6. ACKNOWLEDGMENTS

This work was partially supported by NSF grants DMS-2145384 to PC and DMS-2204349 to AK. The core of the paper was chewed through during the 2023 Moab Topology Conference. We thank the organizers Nathan Geer, Mark Hughes, Maggie Miller and Matt Young for all the fruit.

m	Seifert genus	Degree of cover q	Multiple of η_1 which bounds in in $H_1(\Sigma_q)$	$\text{lk}(\eta^1, \eta^2), \text{lk}(\eta^1, \eta^3), \dots, \text{lk}(\eta^1, \eta^q)$
0	1	2	9	4/9
0	1	3	7	2/7, 2/7
0	1	4	45	2/9, 8/45, 2/9
0	1	5	31	6/31, 4/31, 4/31, 6/31
1	3	2	289	120/289
1	3	3	151	40/151, 40/151
1	3	4	1875	60/289, 3036/18785, 60/289
1	3	5	7481	1350/7481, 896/7481, 896/7481, 1350/7481
2	5	2	9801	4060/9801
2	5	3	3457	912/3457, 912/3457
2	5	4	8830701	2030/9801, 1405300/8830701, 2030/9801
2	5	5	2042281	369248/2042281, 239272/2042281, 239272/2042281, 369248/2042281

TABLE 5. Linking numbers for Example 3: patterns with winding number 0 determined by the two-bridge slice knots P_m in Figure 10.

REFERENCES

- [1] Final report. In *Synchronizing Smooth and Topological 4-Manifolds*. BIRS, 2016.
- [2] Selman Akbulut and Robion Kirby. Branched covers of surfaces in 4-manifolds. *Mathematische Annalen*, 252:111–131, 1980.
- [3] Joan S Birman and Julian Eisner. *Seifert and Threlfall, A Textbook of Topology*. Academic Press, 1980.
- [4] Patricia Cahn, Elise Catania, Sarangoo Chingee, Olivia Del Guercio, and Jack Kendrick. Dihedral linking invariants. *arXiv preprint arXiv:2112.14790*, 2021.
- [5] Patricia Cahn and Alexandra Kjuchukova. Linking numbers in cyclic covers. https://github.com/patriciacahn/cyclic_covers_linking.
- [6] Patricia Cahn and Alexandra Kjuchukova. Computing ribbon obstructions for colored knots. *Fundamenta Mathematicae*, 253(2), 2021.
- [7] Patricia Cahn and Alexandra Kjuchukova. Linking numbers in three-manifolds. *Discrete & Computational Geometry*, 66(2):435–463, 2021.
- [8] Sylvain E. Cappell and Julius L. Shaneson. Invariants of 3-manifolds. *Bulletin of the American Mathematical Society*, 81(3):559–562, 1975.
- [9] Jae Choon Cha and Ki Hyoung Ko. Signatures of links in rational homology spheres. *Topology*, 41(6):1161–1182, 2002.
- [10] Christian Geske, Alexandra Kjuchukova, and Julius L Shaneson. Signatures of topological branched covers. *International Mathematics Research Notices*, 2021(6):4605–4624, 2021.
- [11] Matthew Hedden and Juanita Pinzón-Caicedo. Satellites of infinite rank in the smooth concordance group. *Inventiones mathematicae*, 225(1):131–157, 2021.
- [12] Alexandra Kjuchukova. Dihedral branched covers of four-manifolds. *Advances in Mathematics*, 332:1–33, 2018.
- [13] Christoph Lamm. Symmetric union presentations for 2-bridge ribbon knots. *Journal of Knot Theory and Its Ramifications*, 30(12), 2022.
- [14] Tye Lidman, Allison N Miller, and Juanita Pinzón-Caicedo. Linking number obstructions to satellite homomorphisms. *arXiv preprint arXiv:2207.14198*, 2022.
- [15] Allison Miller. Homomorphism obstructions for satellite maps. *Transactions of the American Mathematical Society, Series B*, 10(08):220–240, 2023.
- [16] Kenneth A Perko. *An invariant of certain knots*. PhD thesis, Department of Mathematics, 1964.
- [17] Józef Przytycki and Akira Yasuhara. Linking numbers in rational homology 3-spheres, cyclic branched covers and infinite cyclic covers. *Transactions of the American Mathematical Society*, 356(9):3669–3685, 2004.
- [18] Kurt Reidemeister. *Knotentheorie*, volume 1. Springer-Verlag, 2013.

7. APPENDIX

We explain how to use the code in [5] to apply Theorems 2 and 3. See Figure 11 for a concrete example.

The first step is to fix an oriented diagram of the link $K \cup \eta \cup \gamma$ where K has writhe 0. Fix a point on K and label the corresponding arc by k_0 . Proceed in the direction of the orientation of K and assign to consecutive arcs labels k_i , increasing the subscript each time the knot encounters an overpass. See Figure 1 for reference. Proceed similarly with η and γ , assigning labels η_i and γ_i , respectively.

Next, we input the diagram into the computer, which amounts to recording the following information: the number of components; the sign of each crossing; the over-strand of each crossing. For the latter, this means specifying a component of the link³ and an arc on this component. The signs are recorded as “1” and “-1,” and the over-strands are recorded as by specifying which link component the over-strand belongs to, and which arc it is of this component.

To record the above information, as well as to perform computations, we use the following functions:

- (1) `Link_component(, ,)` introduces a component to the link diagram. It takes as input: an integer c , the number of components in the diagram; a list of 1-s and -1-s, the signs of crossings along this new component; a list of integer pairs $[a, b]$ where $a \in \{0, 1, \dots, n-1\}$ specifies the component containing the overstrand at each crossing, and b specifies the arc on this component that is the overstrand. Each new component should be named. In Figure 11, the names used are “knot” and “pb_1”.
- (2) `diagram(c, m)` takes as input two integers: c is the number of components in the link diagram; $m \in \{0, 1, \dots, m-1\}$ specifies which component is the branch curve.
- (3) `diagram.add_component` introduces a component, among the ones created in (1), to the diagram.
- (4) $q \in \mathbb{N}$ specifies the degree of the cover.
- (5) `cover = cyclic_cover(q, diagram)` generates the combinatorial data encoding the cell structure described in Section 2.
- (6) `cover.two_chain(a, b)` prints the coefficients of 2-cells the 2-chain found in Theorem 2, whose boundary is the b -th lift of the a -th component of the link diagram. The two cells paired with these coefficients are ordered as follows:

$$(x_0^1, \dots, x_0^q, x_1^1, \dots, x_1^q, \dots, x_{n-1}^1, \dots, x_{n-1}^q)$$

- (7) `cover.linking_number(a, i, b, j)` prints the linking number between the i -th lift of the a -th component and the j -th lift of the b -th component of the link.

³Note that we have stated our theorems for the case of two pseudo-branch curves, and we focus on applications involving a single pseudo-branch curve, η . However, the implementation of our algorithm allows for computing linking numbers between lifts of more than two pseudo-branch curves.

```

In [1]: load('./cyclic_linking_numbers.sage')

In [2]: #(3,1) cable

knot=Link_Component(2,[1,1,1,1,1],[[1,0],[0,0],[1,0],[0,0],[1,0],[0,0]])
pb_1=Link_Component(2,[1,1,1],[[0,1],[0,3],[0,5]])
diagram=Link_Diagram(2,0)
diagram.add_component(knot)
diagram.add_component(pb_1)
q=3

In [3]: cover=Cyclic_Cover(q,diagram)

In [4]: for i in range(1,q+1):
         print(cover.two_chain(1,i))

(0, 0, 0, -1, 0, 1, -1, 0, 1, -1, 1, 0, -1, 1, 0, 0, 0, 0)
(0, 0, 0, 1, -1, 0, 1, -1, 0, 0, -1, 1, 0, -1, 1, 0, 0, 0)
(0, 0, 0, 0, 1, -1, 0, 1, -1, 1, 0, -1, 1, 0, -1, 0, 0, 0)

In [5]: for i in range(1,q+1):
         for j in range(1,q+1):
             if i!=j and i<j:
                 print("linking of pb lift ",i,"with pb lift ",j)
                 print(cover.linking_number(1,i,1,j))

linking of pb lift 1 with pb lift 2
1
linking of pb lift 1 with pb lift 3
1
linking of pb lift 2 with pb lift 3
1

```

FIGURE 11. Computing the linking numbers between lifts of η for the $(3, 1)$ cable.